

A Comparison of Cytotoxic and Genotoxic Damages Induced by 254 Nm and 365 Nm Radiation: *Allium Cepa* L. Model

Kültiğın ÇAVUŞOĞLU

Giresun University: Giresun Universitesi

Tuğçe Kalefetoğlu Macar (✉ tkmacar@gmail.com)

Giresun Universitesi, Şebinkarahisar School of Applied Sciences, Department of Food Technology

Oksal MACAR

Giresun University: Giresun Universitesi

Dilek ÇAVUŞOĞLU

Isparta Uygulamalı Bilimler Universitesi

Emine YALÇIN

Giresun University: Giresun Universitesi

Research Article

Keywords: *Allium cepa*, genotoxicity, meristematic cell damage, oxidative damage, radiation, UV.

Posted Date: May 10th, 2021

DOI: <https://doi.org/10.21203/rs.3.rs-412704/v1>

License: © ⓘ This work is licensed under a Creative Commons Attribution 4.0 International License.

[Read Full License](#)

Abstract

Living organisms are increasingly exposed to ultraviolet (UV) rays of solar radiation, both due to the thinning of the ozone layer and the widespread uses in sterilization processes. The present study was conducted with the purpose of evaluating the damages of UV-A and UV-C radiations in *Allium cepa* L. roots. Three groups were formed from *Allium* bulbs, one of which was the control group. One of the other groups was exposed to 254 nm (UV-C) and the other to 365 nm (UV-A) UV. Growth retardation effect of UV was investigated with respect to germination percentage, total weight gain and root elongation, while genotoxicity arisen from UV exposure analyzed using mitotic index (MI) and chromosomal aberrations (CAs) including micronucleus (MN) frequency. Oxidative stress due to UV application was investigated based on the accumulation of malondialdehyde (MDA) and the total activities of superoxide dismutase (SOD) and catalase (CAT) enzymes. Also, meristematic integrity of the UV treated roots was controlled. UV treatments caused significant changes in all parameters compared to the control, but all effects were much more prominent in 254 nm UV-exposed group. This study clearly revealed that UV exposure triggered growth inhibition, genotoxicity, oxidative stress and meristematic cell damages in *A. cepa* roots depending on the wavelength.

1. Introduction

Sterilization technology, which has an important place for the healthy sustainability of our daily life, has gained a much more vital importance with the recent SARS-CoV-2 pandemic. In addition to being used in the decontamination processes of foods, medicines and hospital equipment, it is utilized to combat infections that may arise from water and sewerage. Chemicals that are frequently used for sterilization have disadvantages such as causing modifications in the features of the targets, generating hazardous substances and leaving residue (Mori et al. 2007; Lindblad et al. 2020). On the other hand, ultraviolet (UV) has many advantages such as not remaining in water, having slight effects on the nature and not producing drug-resistance in microorganisms (Mori et al. 2007). In addition to artificial sources such as UV emitting fluorescent lamps and mercury-vapor lamps, sunlight contains distinct UV classes. UV-A, UV-B and UV-C are types of radiations exist in sunlight with wavelengths of 315–400 nm, 280–315 nm and 200–280 nm, respectively (Kaidzu et al. 2019). Both the thinning of the ozone layer (Bernhard et al. 2020) and the increased use of UV in sterilization treatments cause people to be exposed to excessive amounts of UV radiation.

UV radiation, which can be easily absorbed by intracellular molecules such as amino acids, nucleic acids and membrane polypeptides, causes damages to living organisms in case of high exposure. It is defined as a “complete carcinogen” due to its non-selective deleterious properties and mutagenicity. In addition to its oxidative damage initiating effect, it is a definite tumor initiator and tumor promoter as a replication-, transcription- and translation-preventive agent (D’Orazio et al. 2013; Roy 2017). Because 253.7 nm wavelength is the optimal UV absorption efficiency of DNA, 254 nm UV (UV-C) emitting UV lamps exhibit extraordinary germicidal capacity (Coohill and Sagripanti 2008). On the other hand, UV-A, including 365 nm wavelength, accounts for 6.3% of solar radiation reaching the Earth and is the least injurious

component of UV radiation (Rahimzadeh et al. 2011). Recently, the effectiveness of UV-A and UV-C irradiation against SARS-CoV-2 has been tested and it has been shown that UV-A irradiation has a much lower efficiency in inactivation viruses (Heilingloh et al. 2020). Owing to its sub-lethal outcomes such as protein denaturation, oxidative stress and retardation in growth and energy metabolism, UV-A has been still used for disinfection studies especially in conjunction with other sterilization processes (Jeon and Ha 2018).

In order to determine the alterations arisen from mutagens and carcinogens, the organism being tested should have a steady mitotic activity (Tedesco and Laughinghouse IV 2012). In this regard, *Allium cepa* L. is an ideal model organism due to its rapid growth rate of its roots. Therefore, *Allium* bioassay offers a versatile, convenient and practical test system that is often utilized to assess the possible genotoxicity and cytotoxicity of environmental contaminants (Kalefetoğlu Macar et al. 2020; Macar 2020; Öztürk et al. 2020). An important reason for choosing the *Allium* model is that this organism has an excellent correlation with mammalian test systems (Srivastava and Singh 2020).

UV radiation, which is used excessively for pathogen control, causes a gradual enhancement in the incidence of post-exposure disease cases. This study aimed to reveal the effects of UV radiation types on *A. cepa* and their mechanism of action from various aspects. Genotoxic potentials of UV-A and UV-C radiations were analyzed using MN and other CAs frequencies as well as MI, whereas germination rate, root elongation and weight increase were selected as growth inhibition indicators. Additionally, oxidative stress-inductive effects of UV radiations were assessed via antioxidant enzyme activities [SOD (EC 1.15.1.1) and CAT (EC 1.11.1.6)] and MDA content. Meristematic cell damages generated from UV exposure were also monitored.

2. Materials & Methods

2.1. Preparing the test material and UV irradiation procedure

A. cepa bulbs purchased from a grocery store in Giresun were cleansed from their old roots and outermost dry scales in the laboratory. Bulbs were separated into three groups (Control, UV₂₅₄ and UV₃₆₅) of 50 individuals each after weighing the initial weights (5.42–5.65 g). Basal plates of bulbs in the control group were kept in contact with tap water during the experiment. On the other hand, UV₂₅₄ and UV₃₆₅ groups were irradiated 254 nm UV and 365 nm UV radiations, respectively. A UVGL-58 Handheld UV Lamp was used for UV implementations. UV radiation treatments were applied to the relevant groups (UV₂₅₄ and UV₃₆₅) from a distance of 20 cm from the top of beakers containing bulbs that contacted with tap water. The test was carried out at room temperature and ended after 72 hours.

2.2. Growth retardation analysis

At the end of the test period, the final weights of the bulbs were noted and the total weight increase was established by calculating the difference between the final weight and the initial weight of the bulbs.

Sprouting of adventitious roots from the basal plate was considered as “germination” to determine germination rates of the groups. The root lengths were measured with a ruler at the end of the experiment to determine the effect of the treatments on the root elongation.

2.3. Genotoxicity assessment

1 cm long root tips were used to understand the genotoxicity level generated by UV treatments. Root tips were kept in 1:3 ratio of acetic-alcohol solution for 1 day following a 4 hours long saturated para-dichlorobenzene solution pretreatment (Hill and Myers 1945). Root pieces were hydrolyzed for 14 minutes in a 60°C water bath in 1 N HCl sufficient to cover the roots completely. Following this process, the root pieces, which were thoroughly rinsed with tap water, were stained with Feulgen for 1.5 hours. The staining procedure was terminated by washing the roots under continuously running tap water for 10 minutes. Root tips were crushed in 1 drop of acetic acid (Sharma and Gupta 1982). MI, CAs and MN, used as indicators of genotoxicity, were scored under a research microscope (Olympus CX41) at 500X magnification. A digital camera (Olympus C-5060) was utilized to photograph the slides. For each group, totally 1,000 cells were screened to score CAs incidences including MN, while totally 10,000 cells were taken into consideration to score MI. CAs, MN and MI analyzes were performed by scanning random areas from 10 different slides prepared separately for each group. MI was evaluated as a marker expressing the ratio of cells in mitosis to the total number of cells. Criteria mentioned by Fenech et al. (2003) were used to distinguish MN from parent cell nuclei.

2.4. Determination of MDA level and the total activities of SOD and CAT enzymes

The modified protocol of Heath and Packer (1968) was used to evaluate the accumulation of MDA, a product indicating fatty acid peroxidation in biological membranes. 0.2 g frozen roots were prepared for homogenization in 4 ml of 5% trichloroacetic acid solution by grinding until they became flour. The samples were then centrifuged (15 minute: 12,000 rpm: 25°C). 2 ml of supernatant was mixed with 2 ml of 0.5% thiobarbituric acid prepared in 20% trichloroacetic acid solution. The freshly prepared mixture was heated in a water bath to allow the reaction to take place at 96°C for 30 minutes. The tubes were then moved to the ice bath for cooling. The samples were centrifuged (5 minute: 10,000 rpm: 25°C) and the absorbance of the supernatant fraction at 600 nm and 532 nm was recorded through a spectrophotometer (Shimadzu UV–Vis spectrophotometer / Mini-1240). 600 nm absorbance was subtracted from 532 nm absorbance for omitting non-specific turbidity. MDA concentrations were calculated utilizing the extinction coefficient ($155 \text{ mM}^{-1} \text{ cm}^{-1}$).

SOD and CAT enzymes were extracted pursuant to the same assay mentioned by Zou et al. (2012). 0.5 g segments from roots were weighed and chilled in liquid nitrogen. Samples that were crushed with ice-cold pestle in extraction buffer (sodium phosphate buffer: 0.05 M, pH 7.5) were then centrifuged (20 minute: 14,000 rpm: +4°C). The supernatant collected from the homogenates contained both SOD and CAT enzymes.

The total SOD activity was assayed according to Beauchamp and Fridovich (1971). 0.01 ml of supernatant was added to 1.5 ml of sodium phosphate buffer (0.05 M: pH 7.8) previously mixed with 0.28 ml of distilled water, 0.3 ml of riboflavin (20 μM), 0.3 ml of methionine (130 mM), 0.3 ml of nitroblue tetrazolium chloride (750 μM), 0.3 ml of EDTA- Na_2 (0.1 mM) and 0.01 ml of polyvinylpyrrolidone (4%). 375 $\mu\text{mol m}^{-2} \text{s}^{-1}$ fluorescent light was exposed to the assay mixtures containing SOD enzyme for 15 minute. The absorbance at 560 nm was spectrophotometrically measured (Shimadzu UV-Vis spectrophotometer / Mini-1240).

The total CAT activity was assayed according to Zhang et al (2005). 0.2 ml of supernatant was added to sodium phosphate buffer (0.05 M: pH 7.8) previously mixed with hydrogen peroxide (0.1 M) and distilled water. Decline of the absorbance spectrophotometrically (Shimadzu UV-Vis spectrophotometer / Mini-1240) read at 240 nm reflected the enzymatic consumption of hydrogen peroxide. All procedures for MDA, SOD and CAT analysis were performed for three times.

2.5. Determination of meristematic cell damages

Meristematic cell damages caused by UV applications were investigated using the cross-sections of decapitated roots. 1 ml of methylene blue (1%) was utilized to stain the cross-sections. Slides were analyzed for meristematic cell integrity under a research microscope (Olympus CX41) at 500X magnification. A digital camera (Olympus C-5060) was utilized to photograph the slides.

2.6. Statistics

Data obtained from the analyses were subjected to ANOVA and Duncan's tests to assess the significance of differences ($p < 0.05$). Tables were presented to indicate the mean and standard deviation.

3. Results & Discussion

The first step was to check germination success, to investigate the UV-induced growth regression (Table 1). UV treatments at 254 nm and 365 nm resulted in 33% and 30% reduction in the germination percentages of the bulbs, respectively. Root elongation levels in UV_{254} and UV_{365} groups decreased by 87% and 53% compared to the control. 254 nm and 365 nm UV administrations inhibited the weight gains of the groups by 81% (UV_{254}) and 52% (UV_{365}), respectively. Light is a crucial factor for a healthy growth of plants and the harmful region of solar radiation may cause metabolic damages those can result in devastating effects on plant growth. Hamid and Jawaid (2011) reported that pretreatments with UV-A and UV-C radiations stimulated the germination and growth of Mung bean through auxin biosynthesis. It has already been known that UV-C radiation improves the seed quality and germination in crop seeds prior to sowing, owing to its antifungal capacity (Ferreira et al. 2018). On the other hand, our results were in line with the study of Rahimzadeh et al. (2011) who revealed that the growth inhibition effect of UV-C was much more severe than that of UV-A in *Satureja hortensis* seedlings. Hernandez-Aguilar et al. (2020) reported that UV-C radiation may cause tissue deteriorations affecting growth of *Phaseolus vulgaris* seedlings depending on time. In addition, Foroughbakhch Pournavab et al. (2019) demonstrated that

different regions of UV radiation including UV-C caused remarkable damages in germination and growth in pine, soybeans, sunflower and wheat. Even though responses of below-ground tissues of plants to UV remains unclear, Zhang et al. (2020) suggested that UV-B radiation reduced the length of meristem and elongation regions of *Arabidopsis thaliana* roots due to a reduction in the number of meristem cells.

Table 1
Effects of UV radiation on growth parameters.

| Groups | Germination Percentage (%) (n = 50) | Root Length (cm) (n = 10) | Weight Gain (g) (n = 10) |
|-------------------|-------------------------------------|---------------------------|---|
| Control | 99 | 6.85 ± 1.78 ^a | + 3.75 ^a (5.50 ± 1.58–9.25 ± 1.96) |
| UV ₂₅₄ | 60 | 0.92 ± 0.53 ^c | + 0.70 ^c (5.65 ± 1.60–6.35 ± 1.77) |
| UV ₃₆₅ | 69 | 3.24 ± 1.22 ^b | + 1.78 ^b (5.42 ± 1.54–7.20 ± 1.82) |

*The means shown with different letters (^{a-c}) in the same column were significant at p < 0.05.

Figure 1 reflects the UV-radiation-induced CAs in *A. cepa* roots. Fragments, vagrants, bridges, sticky chromosomes, unequally distributed chromatins, anaphase multipolarities and vacuole nuclei as well micronuclei formation were among the CAs arisen from UV exposure (Fig. 1, Table 2). MI of the group exposed to 254 nm UV was significantly lower than that of both the control and 365 nm UV-treated group. MI has been used as a consistent marker of cell division rate because of the mito-depressive action of a destructive factor (Siddiqui and Alrumman 2020; Yalçın et al. 2020). In the literature, genotoxicity studies associated with UV irradiation have mostly focused on UV-B region of the spectrum (Kumar and Pandey 2017; Mohajer et al. 2018; Debnath et al. 2020). In a study investigating the repressive effect of UV-A, UV-B and UV-C on mitotic activity in *Phaseolus vulgaris* roots, it was shown that all three UV types reduced the frequency of cell division in bean roots depending on the application time (Bara and Tiganasu 2005). Additionally, Verdes-Teodor et al. (2019) showed that UV-C radiation suppressed cell division in a time-dependent manner in *Cucurbita pepo* root meristems. The present work here clearly demonstrated that MI, a representative of the survival success of cells under the pressure of an environmental constraint, was negatively affected by both UV-A and UV-C radiation. Both UV treatments resulted in a remarkable increase in CAs compared to the control, but the frequency of CAs in the group exposed to 254 nm UV was much higher than that of UV₃₆₅. Ali et al. (2017) stated that UV damages to nucleic acids and membrane lipids through cell toxicity, disorders in cell signaling processes and genetic modifications. Fragment was the most abundant CAs type in UV₂₅₄ and UV₃₆₅. Clastogenicity of the agents are known to induce fragment formation through chromosomal breakages and ultimately MN increase in cells (Hintzsche et al. 2017; Rubeena and Thoppil 2020). MN is a routine test system utilized to detect the clastogenicity and aneugenicity of the pollutants (Hintzsche et al. 2017). As a biomarker of genomic pathology and chromosomal damages, it originates from incorporated fragments or intact

chromosomes separated from the main cell nucleus during the mitotic cycle (Fenech et al. 2020). Our study clearly showed that UV exposure was an apparent “MN-inducer”. Although the increase in MN following 254 nm UV application was extremely significant, the amount of MN caused by 365 nm UV treatment was also remarkable. Indeed, MN frequencies of UV₂₅₄ and UV₃₆₅ were approximately 66.8 times and 43.8 times the control, respectively. Our results were in accordance with the study of Helma et al. (1994) who demonstrated that UV irradiation led to a sharp enhancement in MN incidence of *Tradescantia* cells. In addition, Seven et al. (2015) reported that UV-C exposure triggered a significant elevation in *A. cepa* roots. Vagrant and sticky chromosomes were among the most common CAs generated from UV administrations in *Allium* roots (Table 2). Vagrant formation suggests a spindle failure (Haq et al. 2017), while stickiness occurs due to chromosomal contraction, DNA condensation and dissolution abnormalities in nucleoproteins (Yadav et al. 2019). In accordance with our study, DNA is reported to be a vital key for UV-related genetic anomalies in plants and sticky chromosomes are considered as markers of fatal toxicity (Rojas et al. 1993; Debnath et al. 2020). Data of the present study showed that UV application caused anaphase bridge formation in the root cells of *Allium*. According to Fenech et al. (2020) clastogenic factors induces breaks in DNA chains, resulting in acentric chromosomes and various chromosomal rearrangements. These rearrangements may involve the generation of multi-centric chromosomes those give rise to the appearance of anaphase bridges. Another UV-provoked chromosomal anomaly was unequal distribution of chromatins. Dutta et al. (2018) stated that unequally distributed chromatins were consequences of a failure in disjunction of chromatins and were responsible for the rise in vagrant formation. In our study, anaphase multipolarity and vacuole nucleus were the least frequent CAs induced by UV treatments. Multipolar spindles and supernumerary (amplified) centromeres are the primary causes of multipolar anaphase (Vitre et al. 2020). On the other hand, vacuole nucleus indicates a malfunction in the synthesis of DNA during mitosis (Sutan et al. 2014). Similar to our study, previous studies showed that excessive UV undoubtedly induces genotoxic events in living organisms (Wang and Wang 1999; Atienzar et al. 2000; Molinier et al. 2005; Seven et al. 2015; Ibrahim et al. 2019). While UV radiation is mostly absorbed by DNA in the UV-B and UVC regions of the spectrum, absorption in the UV-A region is much weaker (Kiefer 2007). It is not surprising, then, that 254nm UV had a higher capacity to reduce MI and increase CA formation compared to 365nm UV.

Table 2
Effects of UV radiation on CAs frequency and MI.

| Damages | Control | UV ₂₅₄ | UV ₃₆₅ |
|--|-----------------------------|-----------------------------|-----------------------------|
| MI | 750.80 ± 25.16 ^a | 400.70 ± 12.78 ^c | 524.20 ± 17.46 ^b |
| MN | 0.60 ± 0.76 ^c | 40.10 ± 5.13 ^a | 26.30 ± 2.75 ^b |
| FRG | 0.00 ± 0.00 ^c | 57.30 ± 5.72 ^a | 45.40 ± 4.81 ^b |
| VC | 0.00 ± 0.00 ^c | 44.80 ± 4.86 ^a | 31.90 ± 3.66 ^b |
| SC | 0.16 ± 0.32 ^c | 41.50 ± 4.55 ^a | 30.20 ± 3.52 ^b |
| B | 0.00 ± 0.00 ^c | 30.30 ± 3.48 ^a | 22.60 ± 2.91 ^b |
| UDC | 0.00 ± 0.00 ^c | 24.70 ± 2.94 ^a | 17.50 ± 2.34 ^b |
| MA | 0.00 ± 0.00 ^c | 15.20 ± 1.52 ^a | 9.60 ± 1.16 ^b |
| VN | 0.00 ± 0.00 ^c | 10.60 ± 1.18 ^a | 5.80 ± 0.90 ^b |
| *The means shown with different letters (a-c) in the same line were significant at p < 0.05. MI: mitotic index, MN: micronucleus, FRG: fragment, VC: vagrant chromosome, SC: sticky chromosome, B: bridge, UDC: unequal distribution of chromatin, MA: multipolar anaphase, VN: vacuole nucleus. | | | |

Table 3 reflects the alterations in biochemical parameters related to oxidative stress induced by UV treatments. MDA levels in the groups UV₂₅₄ and UV₃₆₅ raised to approximately 3.4 times and 2.4 times the control, respectively. According to Urban et al. (2016), lipid peroxidation is one of the direct effects of ionizing radiation in plants. As a cytotoxic material, MDA points out both the degree of lipid peroxidation in biological membranes caused by the over-production of reactive oxygen species (ROS) and the efficiency of the stress defense (Skórzyńska 2007; Luo et al. 2019). In our study, much greater increase in MDA content in the 254 nm UV-treated group compared to the 365 nm UV-treated group indicated that UV-C caused a more serious oxidative burst in *Allium* root cells. Similar to our results, Luo et al. (2019) reported a remarkable increase in MDA levels in UV-C radiation-exposed grapes. In another study, UV-C pulses triggered significant increases in MDA contents of tobacco callus in a time-dependent manner (Zacchini and de Agazio 2004). Although Tokarz et al. (2019) reported that UV-A application did not induce a remarkable alteration in MDA content in grass pea, our data on MDA content showed that UV-A exposure disturbed the membrane integrity in *Allium* roots.

UV-mediated oxidative stress may occur due to the direct relation of ionizing radiation with cellular macromolecules including DNA or may be induced by UV-triggered ROS accumulation (Rastogi et al. 2010; De Jager et al. 2017). Since UV exposure is inevitable for plants and UV light has a strong potential for ROS production, plants have evolved functional defense mechanisms including antioxidant enzymes against UV-mediated oxidative imbalance (Chen et al. 2019). SOD and CAT enzymes are among the key members of enzymatic antioxidant defense system. SOD catalyzes the conversion of superoxide radicals

to oxygen and hydrogen peroxide and is the first step in combating ROS. However, for accomplished oxidative stress elimination, the increase in SOD activity should be supported by the enhanced activities of other enzymes such as CAT (Ibrahim et al. 2021). CAT enzyme takes part in the decomposition of hydrogen peroxide into water and oxygen (Foryer and Noctor 2000). The present study showed that UV exposure led to a sharp increase in the total activities of SOD and CAT enzymes. The total SOD activities in the groups UV₂₅₄ and UV₃₆₅ increased to nearly 2.6 times and 1.9 times the control, respectively. In addition, the total CAT activities of UV₂₅₄ and UV₃₆₅ were 2.9-fold and 2.1-fold of the control group. Our results demonstrating the rise in the enzyme activities confirmed Xie et al. (2009), who stated that SOD and CAT enzymes play important roles against UV. On the contrary to our data, Zacchini and de Agazio (2004) reported that CAT activity did not enhance in tobacco callus following UV-C irradiation. On the other hand, in another study, UV-B radiation caused an increase in CAT activity in barley (Mazza et al. 2001). Our data were consistent with Erkan et al. (2008), who demonstrated that UV-C illumination significantly stimulated SOD activity in strawberry fruits. Similarly, SOD and CAT activities in papaya fruits were enhanced following postharvest application of UV-C (Rivera-Pastrana et al. 2014). In our study, the increase in antioxidant enzyme activities associated with CAs accumulation clearly revealed that UV exposure leads to the formation of ROS that also targets DNA and proper cell division. In fact, the main damage target of UV-C on cells is directly the DNA molecule, while the mechanism of damage caused by UV-A radiation is indirect damage of oxidative stress (Qiu et al. 2005). Nevertheless, the antioxidant enzyme activities of the 254 nm UV treated roots in our study were much higher than 365 nm UV radiation exposed group, proving that UV-C also triggered severe levels of ROS accumulation.

Table 3
Effect of UV radiation on biochemical parameters.

| Groups | MDA ($\mu\text{M g}^{-1}$ FW) | SOD (U mg^{-1} FW) | CAT ($\text{OD}_{240 \text{ nm}} \text{ min g}^{-1}$ FW) |
|--|-----------------------------------|---------------------------------|--|
| Control | 8.20 \pm 1.75 ^c | 86.50 \pm 6.84 ^c | 0.31 \pm 0.69 ^c |
| UV ₂₅₄ | 28.20 \pm 3.16 ^a | 227.80 \pm 14.10 ^a | 0.90 \pm 1.12 ^a |
| UV ₃₆₅ | 19.40 \pm 2.83 ^b | 166.90 \pm 09.32 ^b | 0.64 \pm 0.88 ^b |
| *The means shown with different letters (^{a-c}) in the same column were significant at $p < 0.05$. | | | |

The effects of UV exposure on the meristematic tissue monitored microscopically (Table 4, Fig. 2). The severity of the damages was classified as “no damage”, “light damage”, “moderate damage” and “intense damage”. Control treated with tap water throughout the experiment had no kinds of meristematic cell damages. On the other hand, UV-exposed groups exhibited various anomaly types in meristematic tissues including epidermis cell damage, necrosis, giant cell nucleus, cortex cell damage and indistinct transmission tissue (Fig. 2). Epidermis and cortex cell damages were the most frequent damage types in both groups exposed to UV, but the degree of damage was more severe in UV₂₅₄ group. Other disorder types observed in UV₂₅₄ and UV₃₆₅ were at “moderate” and “light” degrees, respectively. In our study, it

was pretty clear that 254 nm UV had a much more destructive effect on meristematic tissue integrity than 365 nm UV.

Table 4
Meristematic cell damages induced by UV radiation.

| Damages | ECD | N | GCN | CCD | ITT |
|-------------------|-----|----|-----|-----|-----|
| Control | - | - | - | - | - |
| UV ₂₅₄ | +++ | ++ | ++ | +++ | ++ |
| UV ₃₆₅ | ++ | + | + | ++ | + |

* ECD: epidermis cell damage, N: necrosis, GCN: giant cell nucleus, CCD: cortex cell damage, ITT: indistinct transmission tissue. (-): no damage, (+): light damage, (++) : moderate damage, (+++): intense damage.

Since the epidermis is a superficial tissue and transmits UV rays to the lower tissues, it was not surprising that there were severe deteriorations in cortex cells as well as in epidermis cells. The malformations in the transmission bundles showed us how deep UV radiation could penetrate tissues. Previous studies have showed that UV-C modifies the root tissues in plants (Kareem et al. 2019). For instance, thickening of epidermal cells is one of the morpho-anatomical defense strategies against UV radiation in plants (DeLucia et al. 1992). Our results showing necrotic zones confirmed the suggestion of Zacchini and de Agazio (2004), who reported that excessive doses of UV radiation lead to an oxidative stress which in turn causes tissue necrosis and retarded plant growth.

4. Conclusion

This study was performed in order to contribute to studies focusing on effective inactivation methods against viruses including SARS-CoV-2. The results of this study demonstrated the harmful effects UV-A and UV-C radiation commonly used in UV sterilizers on *A. cepa*, a recognized model organism. Both types of UV radiation induced growth suppression, genotoxicity, cell membrane damage and meristematic cell injuries. It was pretty noticeable that antioxidant enzyme activities were stimulated in *Allium* roots to suppress oxidative stress caused by UV exposure. Here we report that 254 nm UV had much more deleterious potential than 365 nm UV. Although UV radiation is one of the most advantageous methods for disinfecting or preventing pathogens, data of the present study proved that it can still pose a danger to non-target organisms.

Declarations

Authors' contributions Dr. Kültiğın Çavuşoğlu, Dr. Tuğçe Kalefetoğlu Macar, Dr. Oksal Macar, Dr. Dilek Çavuşoğlu, and Dr. Emine Yalçın carried out the experimental stages, manuscript preparation and statistical analysis.

Availability of data and materials All data and materials generated, utilized or analyzed during this study are included in this published article.

Conflict of Interest No conflicts of interest have been declared by the authors.

Funding Not applicable.

Ethical approval Not applicable.

Consent to participate Not applicable.

Consent to publish All authors whose names appear on the submission approved the version to be published and agree to be accountable for all aspects of the work in ensuring that questions related to the accuracy or integrity of any part of the work are appropriately investigated and resolved.

References

1. Ali A., Rashid MA, Huang QY, Lei CL (2017) Influence of UV-A radiation on oxidative stress and antioxidant enzymes in *Mythimna separata* (Lepidoptera: Noctuidae). *Environ Sci Pollut Res* 24(9):8392-8398
2. Atienzar FA, Cordi B, Donkin ME, Evenden AJ, Jha AN, Depledge MH (2000) Comparison of ultraviolet-induced genotoxicity detected by random amplified polymorphic DNA with chlorophyll fluorescence and growth in a marine macroalgae, *Palmaria palmata*. *Aqua Toxicol* 50(1-2):1-12
3. Bara CI, Tiganasu OG (2005) The action of UV radiation on mitotic index and mitotic division phases at *Phaseolus vulgaris* L. *J Exp Molec Biol* 6:127-132
4. Beauchamp C, Fridovich I (1971) Superoxide dismutase: improved assays and an assay applicable to acrylamide gels. *Anal Biochem* 44:276-287
5. Bernhard GH, Neale RE, Barnes PW, Neale PJ, Zepp RG, Wilson SR, Andrady AL, Bais AF, McKenzie RL, Aucamp PJ, Young PJ, Liley JB, Lucas RM, Yazar S, Rhodes LE, Byrne SN, Hollestein LM, Olsen CM, Young AR, Robson TM, Bornman JF, Jansen MAK, Robinson SA, Ballaré CL, Williamson CE, Rose KC, Banaszak AT, Häder D-P, Hylander S, Wängberg S-Å, Austin AT, Hou W-C, Paul ND, Madronich S, Sulzberger B, Solomon KR, Li H, Schikowski T, Longstreth J, Pandey KK, Heikkilä AM, White CC (2020) Environmental effects of stratospheric ozone depletion, UV radiation and interactions with climate change: UNEP Environmental Effects Assessment Panel, update 2019. *Photochem Photobiol Sci* 19(5):542-584
6. Chen Z, Ma Y, Weng Y, Yang R, Gu Z, Wang P (2019) Effects of UV-B radiation on phenolic accumulation, antioxidant activity and physiological changes in wheat (*Triticum aestivum* L.) seedlings. *Food Biosci* 30:100409
7. Coohill TP, Sagripanti JL (2008) Overview of the inactivation by 254 nm ultraviolet radiation of bacteria with particular relevance to biodefense. *Photochem Photobiol* 84(5):1084-1090

8. De Jager TL, Cockrell AE, Du Plessis SS (2017) Ultraviolet light induced generation of reactive oxygen species. In: Ahmad S (ed) Ultraviolet light in human health, diseases and environment, advances in experimental medicine and biology 996. Springer, Cham, pp 15-23
9. Debnath P, Mondal A, Sen K, Mishra D, Mondal NK (2020) Genotoxicity study of nano Al₂O₃, TiO₂ and ZnO along with UV-B exposure: An *Allium cepa* root tip assay. Sci Total Environ 713:136592
10. DeLucia EH, Day TA, Vogelmann TC (1992) Ultraviolet-B and visible light penetration into needles of two species of subalpine conifers during foliar development. Plant Cell Environ 15(8):921-929
11. D'Orazio J, Jarrett S, Amaro-Ortiz A, Scott T (2013) UV radiation and the skin. Int J Mol Sci 14(6):12222-12248
12. Dutta J, Ahmad A, Singh J (2018) Study of industrial effluents induced genotoxicity on *Allium cepa* L. Caryologia 71(2):139-145
13. Erkan M, Wang SY, Wang CY (2008) Effect of UV treatment on antioxidant capacity, antioxidant enzyme activity and decay in strawberry fruit. Postharvest Biol Tech 48(2):163-171
14. Fenech M, Chang WP, Kirsch-Volders M, Holland N, Bonassi S, Zeiger E (2003) HUMN Project: Detailed description of the scoring criteria for the cytokinesis-block micronucleus assay using isolated human lymphocyte cultures. Mutat Res 534:65-75
15. Fenech M, Knasmueller S, Bolognesi C, Holland N, Bonassi S, Kirsch-Volders M (2020) Micronuclei as biomarkers of DNA damage, aneuploidy, inducers of chromosomal hypermutation and as sources of pro-inflammatory DNA in humans. Mutat Res Rev Mutat Res 786:108342
16. Ferreira CD, Ziegler V, Schwanz Goebel JT, Lang GH, Elias MC, de Oliveira M (2018) Quality of grain and oil of maize subjected to UV-C radiation (254 nm) for the control of weevil (*Sitophilus zeamais* Motschulsky). J Food Process Pres 42:e13453
17. Foroughbakhch Pournavab R, Bacópulos Mejía E, Benavides Mendoza A, Salas Cruz LR, Ngangyo Heya M (2019) Ultraviolet radiation effect on seed germination and seedling growth of common species from Northeastern Mexico. Agronomy 9(6):269
18. Foryer C, Noctor G (2000) Oxygen processing in photosynthesis: Regulation and signaling. New Phytol 146:359-388
19. Hamid N, Jawaid F (2011) Influence of seed pre-treatment by UV-A and UV-C radiation on germination and growth of mung beans. Pak J Chem 1(4):164-167
20. Haq I, Kumar S, Raj A, Lohani M, Satyanarayana GNV (2017) Genotoxicity assessment of pulp and paper mill effluent before and after bacterial degradation using *Allium cepa* test. Chemosphere 169:642-650
21. Heath RL, Packer L (1968) Photoperoxidation in isolated chloroplasts: II. Role of electron transfer. Arch Biochem Biophys 125(3):850-857
22. Heilingloh CS, Aufderhorst UW, Schipper L, Dittmer U, Witzke O, Yang D, Zheng X, Sutter K, Trilling M, Alt M, Steinmann E, Krawczyk A (2020) Susceptibility of SARS-CoV-2 to UV irradiation. Am J Infect Control 48(10):1273-1275

23. Helma C, Sommer R, Schulte-Hermann R, Knasmüller S (1994) Enhanced clastogenicity of contaminated groundwater following UV irradiation detected by the *Tradescantia* micronucleus assay. *Mutat Res Lett* 323(3):93-98
24. Hernandez-Aguilar C, Dominguez-Pacheco A, Tenango MP, Valderrama-Bravo C, Hernández MS, Cruz-Orea A, Ordonez-Miranda J (2020) Characterization of bean seeds, germination, and phenolic compounds of seedlings by UV-C radiation. *J Plant Growth Regul*: 1-14.
25. Hill HD, Myers WM (1945) A schedule including cold treatment to facilitate somatic chromosome counts in certain forage grasses. *Stain Technol* 20:89-92
26. Hintzsche H, Hemmann U, Poth A, Utesch D, Lott J, Stopper H (2017) Fate of micronuclei and micronucleated cells. *Mutat Res Rev Mutat Res* 771:85-98
27. Ibrahim ATA, AbouelFadl KY, Osman AG (2019) Ultraviolet A-induced hematotoxic and genotoxic potential in Nile tilapia *Oreochromis niloticus*. *Photochem Photobiol Sci* 18(6):1495-1502
28. Ibrahim MFM, Ibrahim HA, Abd El-Gawad HG (2021) Folic acid as a protective agent in snap bean plants under water deficit conditions. *J Hortic Sci Biotech* 96(1):94-109
29. Jeon MJ, Ha JW (2018) Efficacy of UV-A, UV-B, and UV-C irradiation on inactivation of foodborne pathogens in different neutralizing buffer solutions. *LWT* 98:591-597
30. Kaidzu S, Sugihara K, Sasaki M, Nishiaki A, Igarashi T, Tanito M (2019) Evaluation of acute corneal damage induced by 222-nm and 254-nm ultraviolet light in Sprague–Dawley rats. *Free Radic Res* 53(6):611-617
31. Kalefetoğlu Macar T, Macar O, Yalçın E, Çavuşoğlu K (2020) Resveratrol ameliorates the physiological, biochemical, cytogenetic, and anatomical toxicities induced by copper (II) chloride exposure in *Allium cepa* L. *Environ Sci Pollut Res* 27(1):657-667
32. Kareem KA, Olobatoke TJ, Rahaman AA, Mustapha OT (2019) Mutagenic effects of ultraviolet (UV-C) irradiation on the anatomy of three species of *Capsicum*. *Bangladesh J Sci Ind Res* 54(2):111-116
33. Kiefer J (2007) Effects of ultraviolet radiation on DNA. In: Obe G, Vijayalaxmi (eds) *Chromosomal alterations*. Springer, Berlin, Heidelberg, pp 39-53
34. Kumar G, Pandey A (2017) Effect of UV-B radiation on chromosomal organisation and biochemical constituents of *Coriandrum sativum* L. *Jordan J Biol Sci* 10(2):85-93
35. Lindblad M, Tano E, Lindahl C, Huss F (2020) Ultraviolet-C decontamination of a hospital room: amount of UV light needed. *Burns* 46(4):842-849
36. Luo YY, Li RX, Jiang QS, Bai R, Duan D (2019) Changes in the chlorophyll content of grape leaves could provide a physiological index for responses and adaptation to UV-C radiation. *Nord J Bot* 37(4):1-11
37. Macar O (2020) Multiple toxic effects of tetraconazole in *Allium cepa* L. meristematic cells. *Environ Sci Pollut Res* 1-8.
38. Mazza CA, Battista D, Zima AM, Szwarcberg-Bracchitta M, Giordano CV, Acevedo A, Scopel AL, Ballare CL (2001) The effect of solar ultraviolet-B radiation on the growth and yield of barley are

- accompanied by increased DNA damage and antioxidant responses. *Plant Cell Environ* 22:61-70
39. Mohajer S, Taha RM, Mohajer M, Anuar N (2018) UV-B irradiation effects on pigments and cytological behaviour of callus in sainfoin (*Onobrychis viciifolia* Scop.). *Pigm Resin Technol* 47(6):496-501
 40. Molinier J, Oakeley EJ, Niederhauser O, Kovalchuk I, Hohn B (2005) Dynamic response of plant genome to ultraviolet radiation and other genotoxic stresses. *Mutat Res-Fund Mol Mech Mut* 571(1-2):235-247
 41. Mori M, Hamamoto A, Takahashi A, Nakano M, Wakikawa N, Tachibana S, Ikehara T, Nakaya Y, Akutagawa M, Kinouchi Y (2007) Development of a new water sterilization device with a 365 nm UV-LED. *Med Biol Eng Comput* 45(12):1237-1241
 42. Öztürk G, Çavuşoğlu K, Yalçın E (2020) Dose–response analysis of potassium bromate–induced toxicity in *Allium cepa* L. meristematic cells. *Environ Sci Pollut Res* 27(34):43312-43321
 43. Qiu X, Sundin GW, Wu L, Zhou J, Tiedje JM (2005) Comparative analysis of differentially expressed genes in *Shewanella oneidensis* MR-1 following exposure to UVC, UVB, and UVA radiation. *J Bacteriol* 187(10):3556-3564
 44. Rahimzadeh P, Hosseini S, Dilmaghani K (2011) Effects of UV-A and UV-C radiation on some morphological and physiological parameters in Savory (*Satureja hortensis* L.). *Ann Biol Res* 2(5):164-171
 45. Rastogi RP, Kumar A, Tyagi MB, Sinha RP (2010) Molecular mechanisms of ultraviolet radiation-induced DNA damage and repair. *J Nucleic Acids* 592980.
 46. Rivera-Pastrana DM, Gardea AA, Yahia EM, Martínez-Téllez MA, González-Aguilar GA (2014) Effect of UV-C irradiation and low temperature storage on bioactive compounds, antioxidant enzymes and radical scavenging activity of papaya fruit. *J Food Sci Technol* 51(12):3821-3829
 47. Rojas E, Herrera LA, Sordo M, Gonsebatt ME, Montero R, Rodriguez R, Ostrosky-Wegman P (1993) Mitotic index and cell proliferation kinetics for identification of antineoplastic activity. *Anticancer Drugs* 4(6):637-640
 48. Roy S (2017) Impact of UV radiation on genome stability and human health. In: Ahmad S (ed) *Ultraviolet light in human health, diseases and environment, advances in experimental medicine and biology* 996. Springer, Cham, pp 207-219
 49. Rubeena M, Thoppil JE (2020) Genotoxicity evaluation of *Cissus latifolia* Lam. and its genoprotective effect on oxidative damage induced by hydrogen peroxide. *Asian J Pharm Clin Res* 13(7):185-191
 50. Seven B, Çavuşoğlu K, Yalçın E, Çavuşoğlu K (2015) *Allium cepa* L.(Amaryllidaceae) kök ucu hücreleri üzerine ultraviyole radyasyonun fizyolojik ve genotoksik etkilerinin araştırılması. *CFD* 36(5):24-31
 51. Sharma PC, Gupta PK (1982) Karyotypes in some pulse crops. *Nucleus* 25:181-185
 52. Siddiqui S, Alrumman S (2020) Cytological changes induced by clethodim in *Pisum sativum* plant. *Bangladesh J Bot* 49(2):367-374

53. Skórzyńska PE (2007) Lipid peroxidation in plant cells, its physiological role and changes under heavy metal stress. *Acta Soc Bot Pol* 1:49-54
54. Srivastava AK, Singh D (2020) Assessment of malathion toxicity on cytophysiological activity, DNA damage and antioxidant enzymes in root of *Allium cepa* model. *Sci Rep* 10(1):1-10
55. Sutan NA, Popescu A, Mihaescu C, Soare LC, Marinescu MV (2014) Evaluation of cytotoxic and genotoxic potential of the fungicide ridomil in *Allium cepa* L. *An Stiint Univ Al I Cuza Iasi* 60(1):5-12
56. Tedesco S, Laughinghouse IV H (2012) Bioindicator of genotoxicity: the *Allium cepa* test. In Srivastava JK (ed) *Environmental contamination*. Intech Open, Rijeka, pp 137-156
57. Tokarz K, Piwowarczyk B, Wysocka A, Wójtowicz T, Makowski W, Golemiec E (2019) Response of grass pea (*Lathyrus sativus* L.) photosynthetic apparatus to short-term intensive UV-A: Red radiation. *Acta Physiol Plant* 41(10):1-7
58. Urban L, Charles F, de Miranda MRA, Aarouf J (2016) Understanding the physiological effects of UV-C light and exploiting its agronomic potential before and after harvest. *Plant Physiol Biochem* 105:1-11
59. Verdes-Teodor A, Vochita G, Creanga D (2019) On some genotoxic effects of UV-C radiation in root meristemes in *Cucurbita pepo* L. *Rom Rep Phys* 71:707
60. Vitre B, Taulet N, Guesdon A, Douanier A, Dossane A, Cisneros M, Maurin J, Hettinger S, Anguille C, Taschner M, Lorentzen E, Delaval B (2020) IFT proteins interact with HSET to promote supernumerary centrosome clustering in mitosis. *EMBO Rep* 21(6):e49234
61. Wang S, Wang X (1999) The *Tradescantia*-micronucleus test on the genotoxicity of UV-B radiation. *Mut Res-Fund Mol Mech Mut* 426(2):151-153
62. Xie Z, Wang Y, Liu Y, Liu Y (2009) Ultraviolet-B exposure induces photo-oxidative damage and subsequent repair strategies in a desert cyanobacterium *Microcoleus vaginatus* Gom. *Eur J Soil Biol* 45(4):377-382
63. Yadav A, Raj A, Purchase D, Ferreira LFR, Saratale GD, Bharagava RN (2019) Phytotoxicity, cytotoxicity and genotoxicity evaluation of organic and inorganic pollutants rich tannery wastewater from a Common Effluent Treatment Plant (CETP) in Unnao district, India using *Vigna radiata* and *Allium cepa*. *Chemosphere* 224:324-332
64. Yalçın E, Çavuşoğlu K, Acar A, Yapar K (2020) In vivo protective effects of *Ginkgo biloba* L. leaf extract against hydrogen peroxide toxicity: cytogenetic and biochemical evaluation. *Environ Sci Pollut Res* 27(3):3156-3164
65. Zacchini M, de Agazio M (2004) Spread of oxidative damage and antioxidative response through cell layers of tobacco callus after UV-C treatment. *Plant Physiol Biochem* 42(5):445-450
66. Zhang H, Jiang Y, He Z, Ma M (2005) Cadmium accumulation and oxidative burst in garlic (*Allium sativum*). *J Plant Physiol* 162(9):977-984
67. Zhang P, Wang R, Wang Y, Xu J (2020) Ultraviolet-B radiation induces cell death in root tips and reprograms metabolism in *Arabidopsis*. *Biol Plant* 64:764-772

Figures

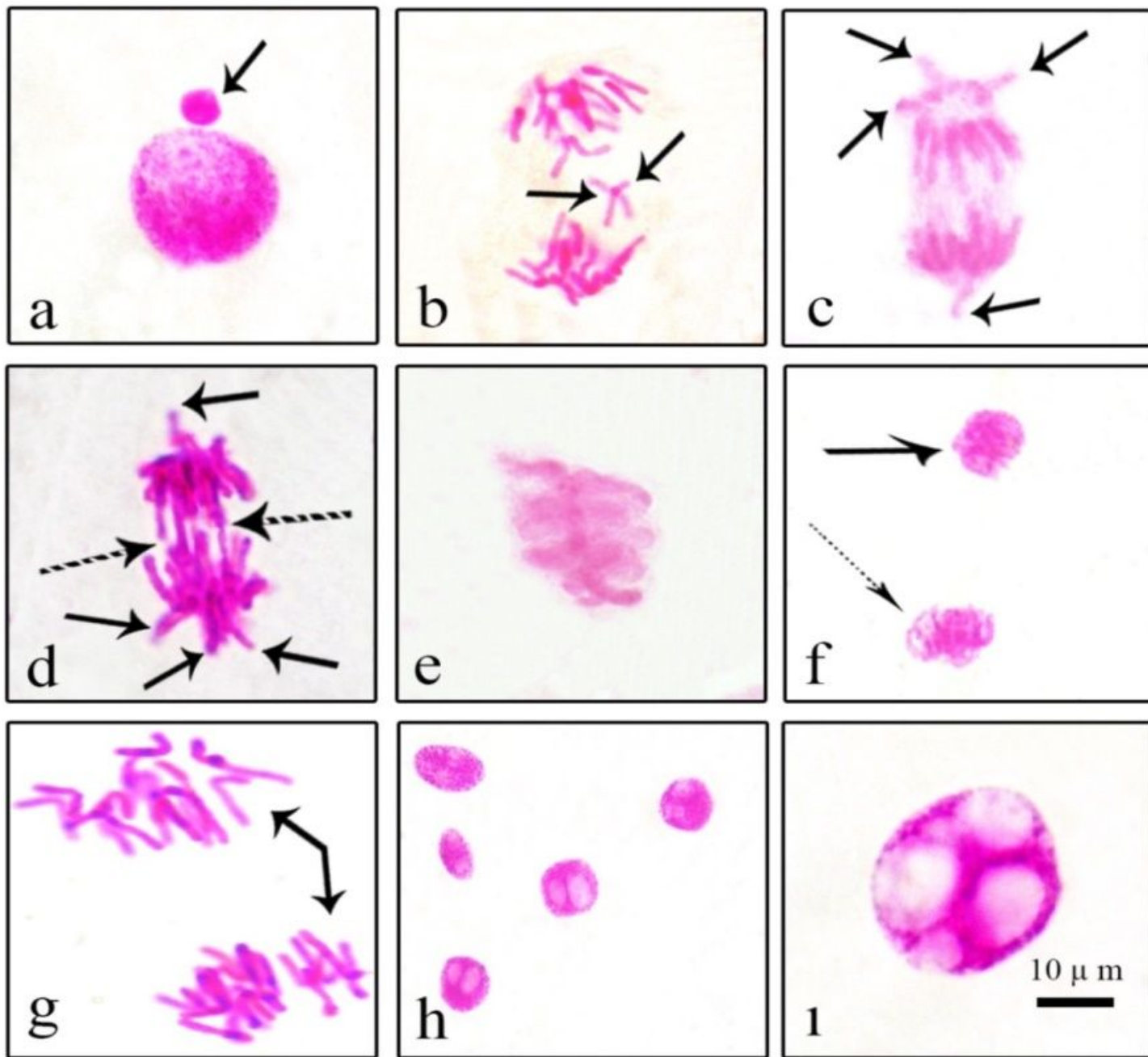


Figure 1

Chromosomal aberrations induced by UV radiation [a: MN at interphase, b: fragment at anaphase, c: vagrant chromosome at anaphase, d: vagrant chromosome (black arrow) and bridges (dotted arrows) at anaphase, e: sticky chromosome, f: unequal distribution of chromatin (dotted arrows) at telophase, g: multipolar anaphase, h, i: vacuole nucleus].

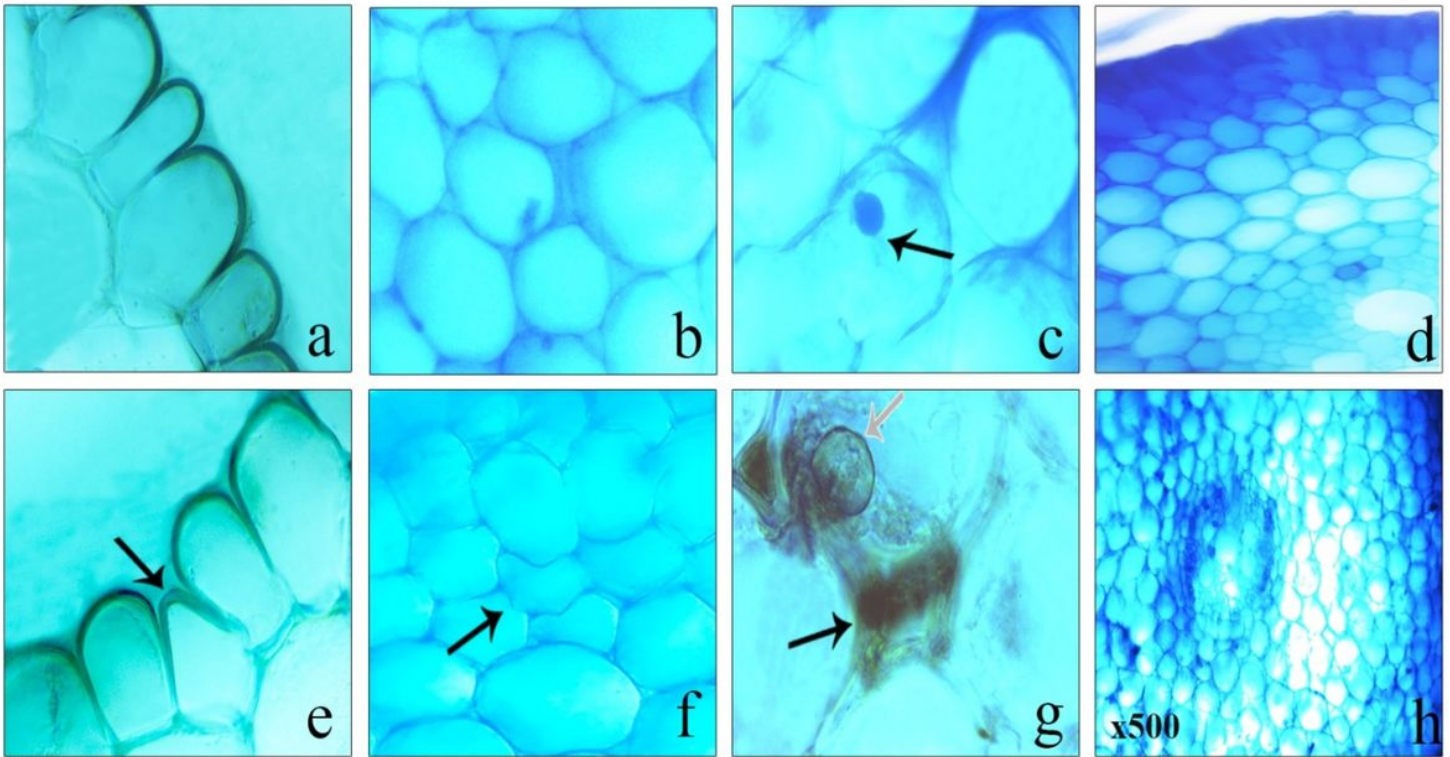


Figure 2

Meristematic cell damages induced by UV [a: normal appearance of epidermis cells, b: normal appearance of cortex cells, c: normal appearance of cell nucleus, d: normal appearance of transmission tissue, e: epidermis cell damage, f: cortex cell damage, g: necrotic zones (black arrow) and giant cell nucleus (white arrow), h: indistinct transmission tissue].